Enhanced Topology of Induction Motor Drive

Ali Abedini[1], Yousef Firouz[2]
1- Electrical & computer engineering, K.N.Toosi University of Technology, Tehran, Iran.
Email: abedini@eetd.kntu.ac.ir
2- Electrical & computer engineering, K.N.Toosi University of Technology, Tehran, Iran.
Email: Yousef.Firouz@gmail.com (Corresponding author)

Received: January 2012 Revised: August 2012 Accepted: October 2012

ABSTRACT:
This paper proposed a new converter topology to drive induction motors. The proposed topology can boost the DC link input voltage in case of DC link voltage shortage without any additional converter. This converter employs two additional switches and one capacitor in each phase compared to conventional converters. Moreover, this new topology brings additional advantages such as less torque and current ripples and lower switching loss. After a discussion of the basic principles of operation, the dynamics of the converter is developed for control purposes. Simulation results are given to illustrate the associated advantages of the proposed converter.

KEYWORDS: Induction Machine Drive, Multilevel Converter, DC Link Fault, Novel Boost Inverter, Volt/Hertz Control Method.

1. INTRODUCTION

New applications of induction machines have increased the demand of AC drives with improved capabilities such as higher speed, and greater power density. To achieve these objectives, much effort is being directed to improve the machine design in order to improve the torque to weight ratio and to reduce the cost [1], [2]. On the converter side, researchers have introduced new control strategies as well as converter topologies to enhance the performance of the drive system.

The new improvements in the control algorithm such as direct torque control and vector control are the results from these efforts [3], [4].

These new applications of electromotive systems require converter topologies, which offer new features. In particular, multi-level converters have been introduced to increase the torque to the volume ratio by allowing operation at an increased voltage while also decreasing the harmonic level in the output [5]-[9]. The most commonly used type of multilevel converters for increasing the input DC link is the cascade converter [10], [11]. However, the DC link voltage balancing, because of the multiple capacitors, is complicated [12]-[14]. On the other hand, in these converters, the output voltage of multilevel converters is limited by DC link voltage.

The proposed circuit presented in this paper is a new type of multi-level circuit, which introduces an additional voltage level only when it is desirable to boost the voltage. The nominal DC link voltage is supplied by rectified input AC voltage and due to faults on the AC side the DC link voltage drops and because of this, the boosting the DC link voltage is required to prevent tripping the motor drive system. Alternatively, in some other cases boosting the DC link voltage may be desirable to ride through the motor over loads such as traction applications.

In [1], [2] Brockerchorhoff introduced a topology for a single phase converter, which is related in this paper. The topology offers the important feature of phase boosting to provide phase balance for a single phase PM motor. In this paper, the concept of [1] is extended and proposes a topology for a three phase converter that has similar features as the single phase version, but can be applied in any type of three phase motor. The key advantage of this new drive topology is the capability to boost the DC link voltage. The results contained in this paper show that the proposed system has superior performance compared to a conventional system.

The organization of this paper is as follows. In next section, the converter topology is shown. The dynamic of the converter is explained in section III. The novel control method is described in section IV and finally, section V indicates simulation results.

2. INVERTER BOOST CIRCUIT

“Fig. 1,” shows the structure of the proposed three phase converter. In this schematic, four switches and one capacitor in parallel with middle switches are used for each inverter leg. Under normal conditions, the capacitor is bypassed by closing the inner switches, and the converter operates similar to conventional converters.

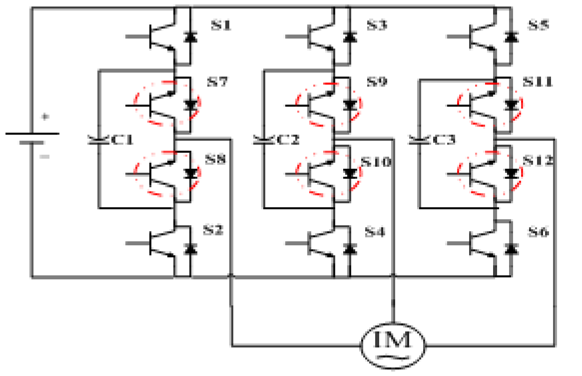

Fig. 1. Circuit structure of the proposed converter

However, for example, when a fault of the AC system occurs and causes the dc link voltage to decrease, the control system will detect the fault and will charge the capacitor by changing the delay time between firing angles of middle switches. Consequently, the voltage of the stator terminals can be controlled to remain constant even at maximum output power and speed.

3. DYNAMIC MODEL OF THE PROPOSED CONVERTER

In order to develop a suitable control system for the converter, a development of the switching dynamics of the converter is necessary. The synchronous d-q frame will be used to analyze the system. It is initially assumed that the voltage of DC link is stiff enough and remains constant during the drive operation.

3.1. Converter model

As discussed in previous sections, in order to the voltage of the stator remains constant during the fault time, the capacitor of each leg should be charged and discharged by the proper switching function of the central switches. The basic concept in this model is based on the charging the capacitors, when the directions of current and voltage for each phase are different and discharge when their directions are the same.

As shown in the “Fig. 2,” during the fault time for one leg, at first the capacitor is charged through the diode when the central switches are open, and capacitor is discharged when one of the central switches is close and another one is open. So,, the voltage of capacitors is added with input DC link when a sag voltage is happened, and because of this, the stator voltage remains constant.

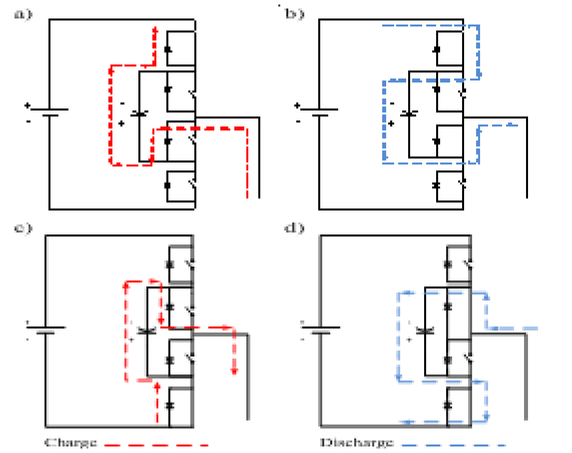

Fig. 2. Charging and discharging process of the capacitor: a) charging when output is connected to positive pole, b) discharging when output is connected to positive pole, c) charging when output in connected to negative pole, d) discharging when output is connected to negative pole.

In this inverter, nine switch states are possible. For example, in “Fig. 3,” s_1,s_8,$s_4 s_9 s_6 s_{11}$ are on.

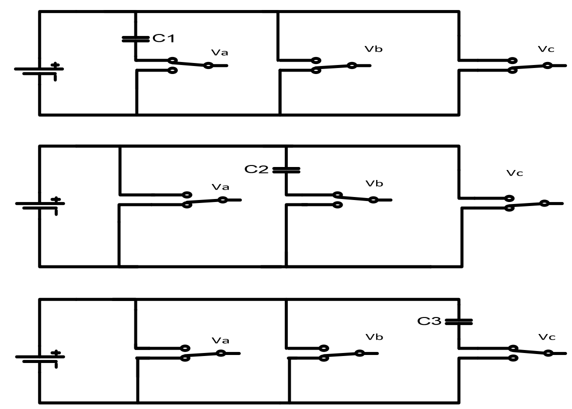

Fig. 3. Switching states

By writing the equation (1) for output voltage of each phase:

$$v_a = (v_{dc} + v_{c1}) * h_a$$
$$v_b = (v_{dc} + v_{c2}) * h_b \qquad (1)$$
$$v_c = (v_{dc} + v_{c3}) * h_c$$

The DC current is:

$$i_{dc} = i_a h_a + i_b h_b + i_c h_c \qquad (2)$$

If the capacitor is in the top of the leg, h =1, otherwise it is equal to zero. The equivalent circuit for this state is shown in “Fig. 4,”.

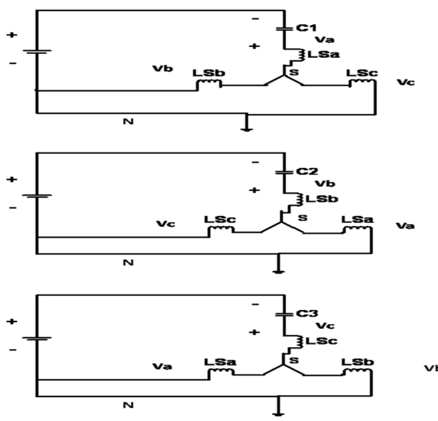

Fig. 4. Equivalent circuit of the converter for the three states involving the additional capacitors

where L_s is stator inductance. In this switching state, phase (b) is parallel with phase (c), and phase (a) is in series. By simplifying the circuit, (Fig. 4) will be derived, and (3) will be obtained.

$$v_{sn} = \frac{1}{3}(v_{an}+v_{bn}+v_{cn}) \quad (3)$$

The assumptions are:

$$v_{c1} = v_{c2} = v_{c3} = v_c \quad (4)$$

From equation (1)-(3), and (4), equation (5) can be derived.

$$v_{sn} = \frac{v_{dc}}{3}(h_a+h_b+h_c) \quad (5)$$

Thus for voltages v_{as}, v_{bs} and v_{cs}

$$v_{as} = (v_{dc}+v_c)h_a - \frac{v_{dc}}{3}(h_a+h_b+h_c)$$
$$= \frac{v_{dc}+v_c}{3}(2h_a - h_b - h_c) \quad (6)$$
$$v_{bs} = \frac{v_{dc}+v_c}{3}(2h_b - h_a - h_c)$$
$$v_{cs} = \frac{v_{dc}+v_c}{3}(2h_c - h_a - h_b)$$

As shown in above equations, the effective inverter dc voltage seen by phase as of the motor is:

$$v_{input} = v_{dc} + v_{ci} \quad i=1,2,3 \quad (7)$$

For analysis of motor drives, the abc axe is transferred to dq0 axe of the same reference frame as the induction motor. The transformation from the abc axes to the dq0 axes in the stator reference frame is given by:

$$\begin{bmatrix} v_{qs} \\ v_{ds} \\ v_{0s} \end{bmatrix} = \begin{bmatrix} 1 & -\frac{1}{3} & -\frac{1}{3} \\ 0 & -\frac{1}{\sqrt{3}} & \frac{1}{\sqrt{3}} \\ \frac{1}{3} & \frac{1}{3} & \frac{1}{3} \end{bmatrix} \begin{bmatrix} v_{as} \\ v_{bs} \\ v_{cs} \end{bmatrix} \quad (8)$$

By inserting the (6) into (8):

$$v_{qs} = \frac{v_{dc}+v_c}{3}(2h_a - h_b - h_c)$$
$$v_{ds} = \frac{v_{dc}+v_c}{\sqrt{3}}(h_c - h_b) \quad (9)$$
$$v_{0s} = 0$$

The dq0 model of a conventional inverter in the stator reference frame was described in [15], [16]. Output voltages and input DC current are:

$$v_{qs} = \frac{2}{\pi} v_i g_{qs}^s \quad (10)$$
$$v_{ds} = \frac{2}{\pi} v_i g_{ds}^s \quad (11)$$
$$\frac{\pi}{3} i_i = i_{qs}^s g_{qs}^s + i_{ds}^s g_{ds}^s \quad (12)$$

where g_{qs}^s and g_{ds}^s are switching functions in the mentioned reference.

For complete modeling of drive system, dq0 model of induction machine should be considered in same reference as the inverter. (13)- (17) indicate detailed dq0 model of induction machine that can be found in [15].

$$\frac{\partial}{\omega_b}\begin{bmatrix} \Delta i \\ \Delta \frac{\omega_r}{\omega_b} \end{bmatrix} = \begin{bmatrix} -X^{-1}G & X^{-1}v_t \\ \frac{1}{2H\omega_b}v_{tt}^T & 0 \end{bmatrix} \begin{bmatrix} \Delta i \\ \Delta \frac{\omega_r}{\omega_b} \end{bmatrix}$$
$$+ \begin{bmatrix} -X^{-1} & 0 \\ 0 & -\frac{1}{2H\omega_b} \end{bmatrix} \begin{bmatrix} \Delta v \\ \Delta T_L \end{bmatrix} \quad (13)$$

where

$$\Delta v^T = [\Delta v_{qs}^e \quad \Delta v_{ds}^e \quad 0 \quad 0] \quad (14)$$
$$\Delta i^T = [\Delta i_{qs}^e \quad \Delta i_{ds}^e \quad \Delta i_{qr}^e \quad \Delta i_{dr}^e] \quad (15)$$
$$v_t^T = [0 \quad 0 \quad -(X_m i_{dso}^e + X_{rr} i_{dro}^e) \quad X_m i_{qso}^e + X_{rr} i_{qro}^e] \quad (16)$$
$$v_{tt}^T = [X_m i_{dro}^e \quad X_m i_{qro}^e \quad -(X_m i_{dso}^e) \quad X_m i_{qso}^e] \quad (17)$$

3.2. Combination of machine and inverter

As discussed above, additional capacitors can be modeled as a capacitor series with DC link voltage and also, the output voltage of the inverter is equal to the input stator voltage of induction machine. According to the "Fig. 5", writing the equation for input DC current gives:

$$i_i = C\frac{dv_c}{dt} \quad (18)$$

By inserting (18) in (12):

$$\frac{dv_c}{dt} = \frac{3}{\pi C} g_{qs}^e i_{qs}^e + \frac{3}{\pi C} g_{ds}^e i_{ds}^e \quad (19)$$

As regards output currents of the inverter is equal to stator current of machine, v_c can be considered as a state space variable, and also it effects on input matrix. Thus regarding to (19), equation (13) can be written as:

$$\frac{\partial}{\omega_b}\begin{bmatrix} \Delta i \\ \Delta \frac{\omega_r}{\omega_b} \\ v_c \end{bmatrix} = \begin{bmatrix} -X^{-1}G & X^{-1}v_t & 0 \\ \frac{1}{2H\omega_b}v_{tt}^T & 0 & 0 \\ F_e & 0 & 0 \end{bmatrix} \begin{bmatrix} \Delta i \\ \Delta \frac{\omega_r}{\omega_b} \\ \Delta v_c \end{bmatrix} + (1/(X_{ss} X'_{rr} X_m^2)) \quad (20)$$
$$\begin{bmatrix} X'_{rr} & 0 & -X_m & 0 & 0 \\ 0 & X'_{rr} & 0 & -X_m & 0 \\ -X_m & 0 & X_{ss} & 0 & 0 \\ 0 & -X_m & 0 & X_{ss} & 0 \\ 0 & 0 & 0 & 0 & -\frac{1}{2H\omega_b}(X_{ss}X'_{rr} - X_m^2) \end{bmatrix} \begin{bmatrix} \frac{2}{\pi}(v_{dc}+v_c) * g_{qs} \\ \frac{2}{\pi}(v_{dc}+v_c) * g_{ds} \\ 0 \\ 0 \\ T_l \end{bmatrix}$$

where F_e is equal to

$$F_e = \left[\frac{3}{\pi C} g_{qs}^e \quad \frac{3}{\pi C} g_{ds}^e \quad 0 \quad 0\right] \tag{21}$$

By solving the equation (20) using numerical methods, the current for each phase and the speed of the rotor can be calculated. The mentioned equation shows that the additional capacitors' effects on transient response of the system and also their voltages are added with input voltage in the input matrix that improves function of the drive system in fault times.

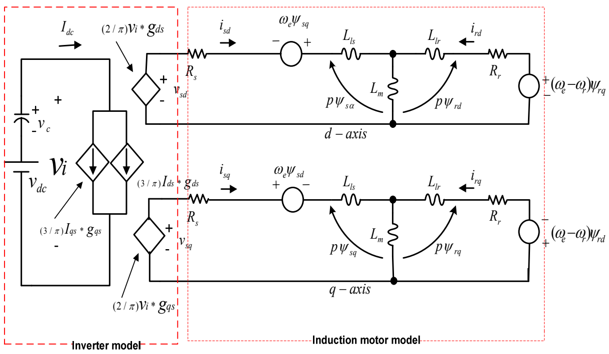

Fig. 5. Equivalent circuit of combination of inverter and machine

4. CONTROL METHOD

"Fig. 6" shows the general control system. The control strategy is a conventional closed loop constant slip control method [17] including the voltage control loop for the additional capacitors. When the voltage of DC link is normal, the converter uses the conventional PWM constant V/Hz strategy. In this mode, the middle switches are turned on and capacitor voltage is zero, consequently. However, when the DC link voltage drops, the voltage sensors detect the fault, and the capacitor will be charged by creating delay in firing angles of middle switches to compensate the voltage drop of the DC link.

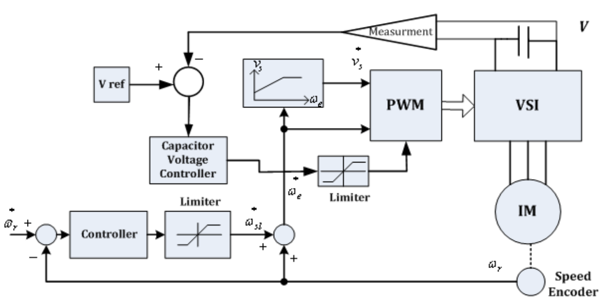

Fig. 6. Control system block diagram.

5. SUMULATION RESULT

To verify the proposed concept, the circuit has been implemented in MATLAB. The input voltage is assumed to be 250 V and at t=1.5 s, it drops to 140 V for two seconds "Fig. 7". The applied torque is 9 N.m. In "Fig. 8", it is obvious that with the new converter, the motor speed follows the reference speed command even when the DC link voltage is abruptly reduced.

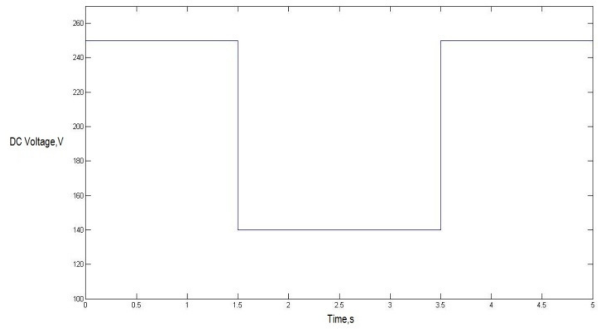

Fig. 7. The DC link voltage.

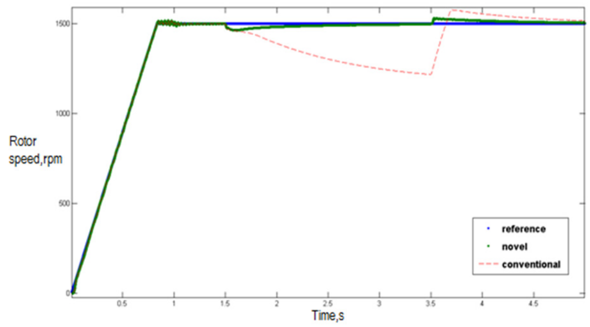

Fig. 8. Comparison of the speed gained from two converters

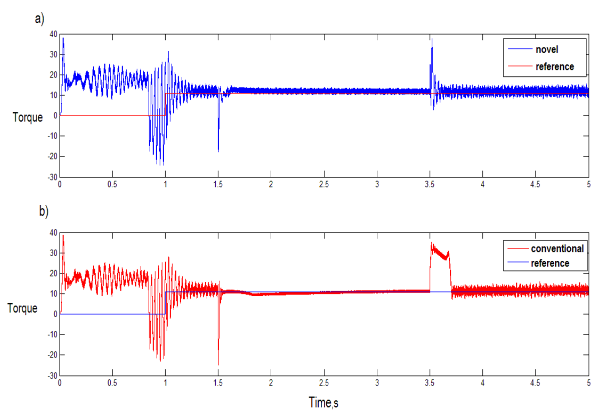

Fig. 9. Comparison of the torque developed in the two converters:
a) Novel, b) Conventional

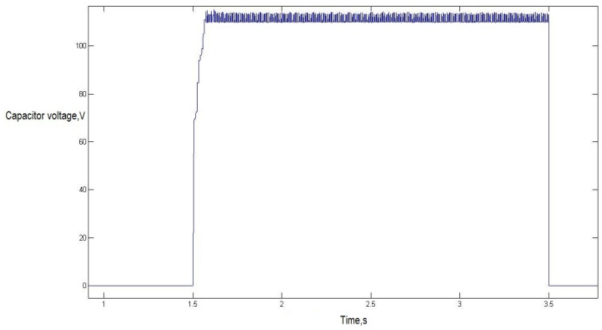

Fig. 10. The capacitor voltage

However, with the conventional converter, there is a large steady-state error. "Fig. 9" shows that in the conventional converter, the developed torque cannot follow its reference command, and it is limited to 13 N.m. Electromagnetic torque oscillates with large amplitude, while in the suggested converter, the oscillation is significant. "Fig. 10 and 11" show that capacitor average voltage remains constant by using proper switching strategy. In this simulation, capacitor voltage is adjusted at 110 Volts.

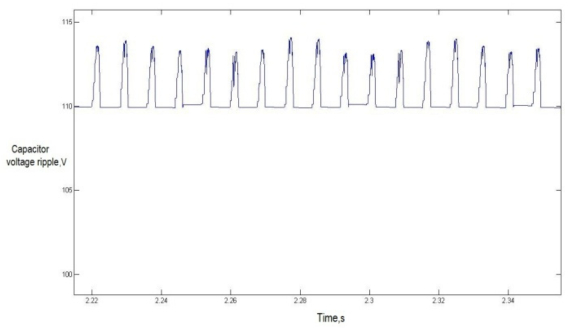

Fig. 11. The capacitor voltage transients during charge and discharge

"Fig. 12" shows the line to line voltage for both converters. Capacitor voltage is added to the stator voltage, clearly and as a result, motor don't sense the voltage sag, and speed remains constant.

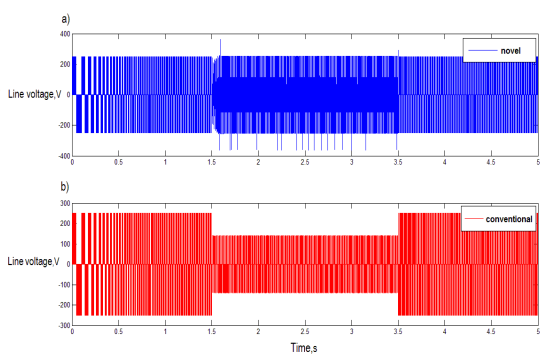

Fig. 12. The line to line motor voltage: a) Novel, b) Conventional

And finally in "Fig. 13", the current of phase A is presented. In the conventional converter, the current magnitude is larger than that of the novel converter in the steady-state. This characteristic is very important because by smaller current, the power dissipation is reduced, and the efficiency is improved.

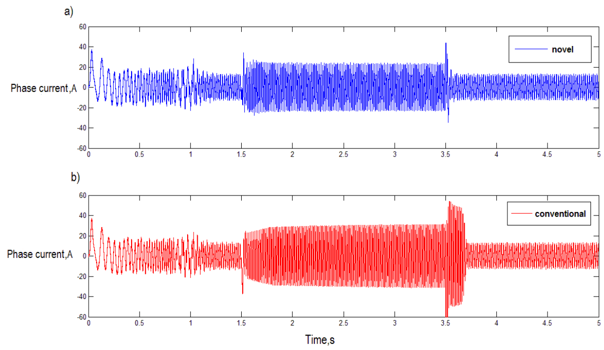

Fig. 13. Comparison of the current drawn by two converters: a) Novel, b) conventional

6. CONCLUSION

In this paper, a new topology for the AC machine's drive was introduced that offered various features such as less loss, and lower ripple current and torque pulsations. The main advantages of the proposed drive compared to conventional drives are the ability of boosting motor terminal voltage during transients, and its capability to ride through input voltage faults. The structure of the drive system was explained, and the system was modeled to evaluate its performance. A control algorithm for the system was proposed, and the proposed system with the suggested control algorithm is simulated in MATLAB, and its performance was shown during different cases. The results show unique ability of the proposed system in compare with conventional ones as described in the introduction.

REFERENCES

[1] P. Brockerchorhoff, M. Ebert, and R. Marquardt, **"A Novel Converter Topology for Permanent Magnet Drive Systems,"** *Power Electronic Specialists Conference, PESC*, 15-19 June 2008, PP 4655-4661.

[2] Philip Brockerhoff, Martin Schulz, **"Control method for a novel converter topology for permanent magnet drives, "** *Applied Power Electronics Conference and Exposition (APEC)*, 21-25 Feb. 2010, PP 1048-2334

[3] Y. Hori, S. Oh, D. Yin, **"A Novel Traction Control fir EV Based on Maximum Transmissible Torque Estimation,Industrial Electronics, "** *IEEE Transaction,* 56 Issue:6 June 2009, PP 0278-0046

[4] C. Shi, J Qui, and R. Lin, **"A Novel Self Commutating Low-Speed Reluctance Motor for Direct-Drive Applications,Industrial Applications,"** *IEEE Transactionon*, Vol. 43, Issue 1, Jan-Feb 2007, PP. 57-65.

[5] L. M. Tolbert, F. Z. Peng, T. G. Habetler, **"Multi-Level Inverters for Electric Vehicle Application,"** *Power Electronics in Transportation*, Vol, no.Oct. 1998, PP 79-84, 22-23

[6] F. Caricchi, F. Crescimbini, T.A. Lipo, **"Converter Topology with Load-Neutral Modulation for Trapezoidal-EMF PM Motor Drives,"** *Power Electronics, IEEE Transaction on*, Vol. 9. No. 2, Mar 1994, PP 232-239.

[7] Y. Sheng, W. Eberle, and L. Yan, **"A Novel Non-Isolated Full Bridge Technology for VRM Application, Power Electronic,"** *IEEE Transaction on*, vol. 23, Issue 1 , Jan 2008, PP. 427-437.

[8] José Rodríguez , Steffen Bernet, BinWu, Jorge O. Pontt, and Samir Kouro, **"Multilevel Voltage-Source-Converter Topologies for Industrial Medium-Voltage Drives,"** *IEEE Transactions On Industrial Electronics*, vol. 54, no. 6, december 2007, pp 0278-0046.

[9] JavadEbrahimi, EbrahimBabaei, and Gevorg B. Gharehpetian, **"A New Multilevel Converter Topology With Reduced Number of Power Electronic Components,"** *IEEE Transactions On Industrial Electronics*, Vol. 59, NO. 2, February 2012, PP 0278-0046.

[10] EbrahimBabaei, SeyedHosseinHosseini, **"New cascaded multilevel inverter topology with minimum number of switches,"** *Published by Elsevier Ltd, Volume 50, Issue 11*, November 2009

[11] Mariusz Malinowski, K. Gopakumar, Jose Rodriguez, Marcelo A. Pérez, **"A Survey on Cascaded Multilevel Inverters,"** *IEEE transaction on industrial electronic, VOL. 57, NO. 7*, JULY 2010, PP 0278-0046.

[12] Leon M. Tolbert, Fang ZhengPeng, TimCunnyngham , John N. Chiasson, **"Charge Balance Control Schemes for Cascade Multilevel Converter in Hybrid Electric Vehicles,"** *IEEE on industrial electronic, VOL. 49, NO. 5*, October 2002, PP 0278-0046.

[13] YingjieHe,YanhuiQiu, Jinjun Liu, Fang Zhuo, Guochun Xiao, **"Theory Analysis of the Hypostasis of DC Voltage Balancing Control for Power Quality Conditioners with Cascaded H-bridge Inverter,"** *Power Electronics Conference (IPEC)*, 21-24 June 2010 PP 11496507.

[14] Chong Han; Huang, A.Q.; Yu Liu; Bin Chen, **"A Generalized Control Strategy of Per-Phase DC Voltage Balancing for Cascaded Multilevel Converter-based STATCOM,"** *Power Electronics Specialists Conference*, PESC 2007, PP 0275-9306.

[15] S. P. Muley, M. V. Aware, **"Modeling and Simulation of a Scalar controlled Induction Motor using combined Inverter Machine Interaction in State Space,"** *Second International Conference on Information and Computing Science*, 2009, DOI 10.1109/ICIC.2009.309.

[16] D. W. Novotny & I. A. Lipo, **Vector control and dynamics of AC drives** (New York, Oxford University, 1996).

[17] P. Vas, **Vector Control of AC Machines** (Clarendon Press, 1994).